

the  $\gamma$ -ray emission. The  $K_{\alpha\beta}$  x-rays originate from the subsequent filling of the holes in the K shell.

17. The Fe foil had a purity of 99.95% and was enriched to 95% in the  $^{57}\text{Fe}$  isotope. Because the atomic mass of the probe atom is 57u and that of the lattice atoms is close to 57u (where u is the atomic mass unit), all results exhibit a systematic deviation from natural Fe (55.86u) in the range of 1 to 2%. This deviation is smaller than the present experimental uncertainty, however it should be considered in all studies with  $^{57}\text{Fe}$ .
18. A. Jayaraman, *Rev. Mod. Phys.* **55**, 65 (1983).
19. V. J. Minkiewicz, G. Shirane, R. Nathans, *Phys. Rev.* **162**, 528 (1967). The DOS is tabulated by H. R. Schober and P. H. Dederichs, in *Landolt-Börnstein*, K.-H. Hellwege and J. L. Olsen, Eds. (Springer-Verlag, Berlin, 1981), vol. III/13a, pp. 53–56.
20. K. S. Singwi and A. Sjölander, *Phys. Rev.* **120**, 1093 (1960).
21. J. D. Althoff, P. B. Allen, R. M. Wentzcovitch, J. A. Moriarty, *Phys. Rev. B* **48**, 13253 (1993).
22. Debye temperatures can be calculated alternatively from the Lamb-Mössbauer factor, the low-tempera-

- ture specific heat, or the low-energy part of the phonon DOS, thus providing slightly different data sets reflecting mainly deviations of the lattice dynamics from a perfect Debye-like behavior.
23. W. Jones and N. H. Marsh, *Theoretical Solid State Physics* (Dover, New York, 1985), vol. 1, p. 237.
24. V. G. Kohn, A. I. Chumakov, R. Rüffer, *Phys. Rev. B* **58**, 8437 (1998).
25. H. K. Mao, Y. Wu, L. C. Chen, J. F. Chu, A. P. Jephcoat, *J. Geophys. Res.* **95**, 21737 (1990).
26. J. Ramakrishnan, R. Boehler, G. H. Higgins, G. C. Kennedy, *J. Geophys. Res.* **83**, 3535 (1978).
27. G. Simmons and H. Wang, *Single Crystal Elastic Constants and Calculated Aggregate Properties* (MIT Press, Cambridge, MA, 1971). The described procedure of calculating  $\nu_p$  and  $\nu_s$  from elastic constants was used also for results from (29, 30).
28. L. Stixrude and R. E. Cohen, *Science* **267**, 1972 (1995); see also (31).
29. P. Söderlind, J. A. Moriarty, J. M. Wills, *Phys. Rev. B* **53**, 14063 (1996).

30. A. Singh, H.-K. Mao, J. Shu, R. J. Hemley, *Phys. Rev. Lett.* **80**, 2157 (1998).
31. H.-K. Mao *et al.*, *Nature* **396**, 741 (1998); *Nature* **399**, 280 (1999).
32. D. Alfé, M. J. Gillan, G. D. Price, *Nature* **401**, 462 (1999).
33. A. Snigirev *et al.*, *Nature* **384**, 49 (1996).
34. A. K. Freund *et al.*, *Proc. SPIE* **3448**, 1 (1998).
35. We thank the Microfluorescence group (ID22) and the Nuclear Resonance group (ID18) of the ESRF for preparation of nuclear resonance station ID22N and for their help during the experiment, A. Snigirev and A. K. Freund for their expert help with the focusing elements, and K. Rupprecht and H. Giefers for their assistance with the measurements. We acknowledge useful discussions with W. B. Holzapfel, R. Rüffer, G. Shen, and W. Sturhahn. Supported by the Bundesministerium für Bildung, Wissenschaft, Forschung und Technologie (project 05 SKBPPA).

11 November 1999; accepted 29 December 1999

## Inhibition of Experimental Liver Cirrhosis in Mice by Telomerase Gene Delivery

Karl Lenhard Rudolph,<sup>1</sup> Sandy Chang,<sup>1,2</sup> Melissa Millard,<sup>1</sup> Nicole Schreiber-Agus,<sup>3</sup> Ronald A. DePinho<sup>1\*</sup>

Accelerated telomere loss has been proposed to be a factor leading to end-stage organ failure in chronic diseases of high cellular turnover such as liver cirrhosis. To test this hypothesis directly, telomerase-deficient mice, null for the essential telomerase RNA (mTR) gene, were subjected to genetic, surgical, and chemical ablation of the liver. Telomere dysfunction was associated with defects in liver regeneration and accelerated the development of liver cirrhosis in response to chronic liver injury. Adenoviral delivery of mTR into the livers of mTR<sup>-/-</sup> mice with short dysfunctional telomeres restored telomerase activity and telomere function, alleviated cirrhotic pathology, and improved liver function. These studies indicate that telomere dysfunction contributes to chronic diseases of continual cellular loss-replacement and encourage the evaluation of "telomerase therapy" for such diseases.

Cirrhosis of the liver is the seventh leading cause of death by disease, affecting several hundred million people worldwide (1). In this chronic disease, a diverse array of hepatotoxins, ranging from chronic viral hepatitis to alcohol, promotes continual hepatocyte destruction that, in turn, stimulates abnormal patterns of hepatocyte regeneration and fibrous scarring over many years (2). The resulting distortion of the liver architecture compromises hepatocyte function, causing systemic life-threatening complications. Left unchecked, this pathological process culmi-

nates in fatal end-stage liver failure, marked by extensive fibrotic replacement and cessation of hepatocyte proliferation (2, 3).

Liver cirrhosis is characterized by the conversion of hepatic stellate cells into activated, myofibroblast like cells (2). It has been postulated that hepatocyte destruction itself serves as an activation signal for this conversion, possibly by the release of insulin-like growth factor or lipid peroxides from apoptotic cells (2). Therefore, factors that govern the survival of hepatocytes could potentially influence stellate cell activation and fibrogenesis.

The second key aspect of terminal liver failure, hepatocyte proliferative arrest, has been linked to several etiologic factors including altered hepatocyte-matrix interactions (2), growth inhibition by abundant transforming growth factor- $\beta$ 1 (TGF- $\beta$ 1) (4), and/or critical telomere shortening. The telomere hypothesis is a particularly appealing one, because sustained hepatocyte turnover accelerates the pace of telomere attrition

in the human cirrhotic liver (5), thereby presumably activating senescence or crisis checkpoints. The importance of telomere maintenance in long-term cellular and organ homeostasis has been experimentally verified in cultured human cells and in telomerase-deficient mice (6, 7). These mice lack the telomerase RNA (mTR) gene and show progressive telomere shortening from one generation to the next. In late-generation mice (e.g. generation 6), telomere dysfunction and genomic instability are associated with impaired proliferation and/or apoptosis in organ systems with high renewal requirements, such as the bone marrow and the gut (8). In contrast, the liver is unperturbed and appears to function and develop normally even in late-generation mTR<sup>-/-</sup> mice (9). Here we use the mTR<sup>-/-</sup> mice to evaluate the role of telomere shortening in chronic liver disease. Liver injury was induced in these animals by three experimental procedures to gauge how telomere shortening influences hepatocyte proliferation, survival, and ultimately predisposition to cirrhosis.

The first system, the albumin-directed urokinase plasminogen activator (Alb-uPA) transgenic mouse, allows investigation of the factors governing hepatocyte regenerative capacity. Alb-uPA expression has been shown to cause widespread hepatocyte death and liver failure in newborn mice (10). However, 60% of hemizygous transgenic mice survive as a result of spontaneous transgene deletion in rare hepatocytes that then clonally expand to reconstitute the entire organ by 3 months of age (11). To assess the impact of loss of telomerase activity and telomere shortening on liver regeneration capacity, we monitored Alb-uPA transgene transmission as well as phenotypic differences in mTR<sup>+/+</sup> mice and successive generations of mTR<sup>-/-</sup> mice (12). Consistent with previous reports (11), we observed transmission rates of 31% for mTR<sup>+/+</sup> and 27% for second-generation (G2) mTR<sup>-/-</sup> mice (Fig. 1A). Because the

<sup>1</sup>Department of Adult Oncology, Medicine and Genetics, Dana-Farber Cancer Institute, 44 Binney Street (M413), and Harvard Medical School, Boston, MA 02115, USA. <sup>2</sup>Department of Pathology, Brigham and Women's Hospital and Harvard Medical School, Boston, MA 02115, USA. <sup>3</sup>Department of Molecular Genetics, Albert Einstein College of Medicine, Bronx, NY 10461, USA.

\*To whom correspondence should be addressed. E-mail: ron\_depinho@dfci.harvard.edu

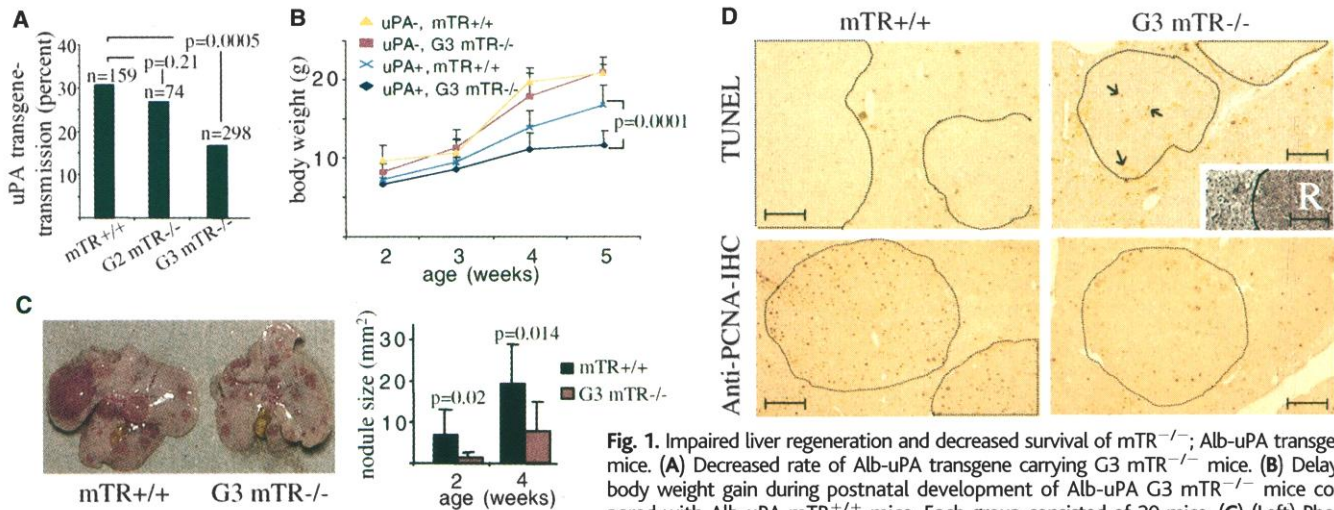


**Fig. 1.** Impaired liver regeneration and decreased survival of mTR<sup>-/-</sup>; Alb-uPA transgenic mice. (A) Decreased rate of Alb-uPA transgene carrying G3 mTR<sup>-/-</sup> mice. (B) Delayed body weight gain during postnatal development of Alb-uPA G3 mTR<sup>-/-</sup> mice compared with Alb-uPA mTR<sup>+/+</sup> mice. Each group consisted of 30 mice. (C) (Left) Photograph of whole livers of 4-week-old Alb-uPA mTR<sup>+/+</sup> mice and Alb-uPA G3 mTR<sup>-/-</sup> mice. (Right) Histogram representation of nodule size in 2- and 4-week-old mice. Each group had 16 to 20 mice. (D) Photomicrographs of TUNEL (top) and PCNA immunohistochemistry (bottom) of liver sections from Alb-uPA mTR<sup>+/+</sup> and Alb-uPA G3 mTR<sup>-/-</sup> mice. Increased numbers of TUNEL-positive cells (arrows) can be seen in the regenerative nodule (circled) in mTR<sup>-/-</sup> mice (bar: 100 μm). (Inset) H&E stain of the border of a regenerative nodule (R, right) and the transgene-expressing liver (left) (bar: 100 μm). PCNA immunostaining (bottom) of regenerating livers demonstrated decreased staining within regenerative nodules (circled) of 5-week-old Alb-uPA G3 mTR<sup>-/-</sup> mice compared with age-matched Alb-uPA mTR<sup>+/+</sup> mice (bar: 100 μm).

Smaller regenerative nodules (red) in Alb-uPA G3 mTR<sup>-/-</sup> liver are apparent. (Right) Histogram representation of nodule size in 2- and 4-week-old mice. Each group had 16 to 20 mice. (D) Photomicrographs of TUNEL (top) and PCNA immunohistochemistry (bottom) of liver sections from Alb-uPA mTR<sup>+/+</sup> and Alb-uPA G3 mTR<sup>-/-</sup> mice. Increased numbers of TUNEL-positive cells (arrows) can be seen in the regenerative nodule (circled) in mTR<sup>-/-</sup> mice (bar: 100 μm). (Inset) H&E stain of the border of a regenerative nodule (R, right) and the transgene-expressing liver (left) (bar: 100 μm). PCNA immunostaining (bottom) of regenerating livers demonstrated decreased staining within regenerative nodules (circled) of 5-week-old Alb-uPA G3 mTR<sup>-/-</sup> mice compared with age-matched Alb-uPA mTR<sup>+/+</sup> mice (bar: 100 μm).

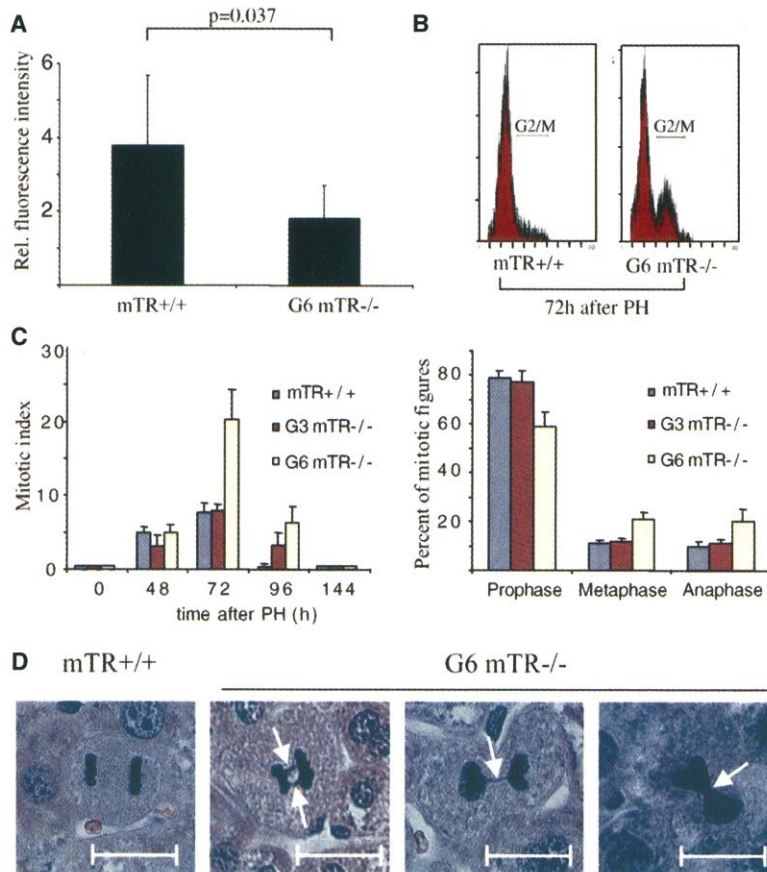


**Fig. 2.** Impaired cell cycle progression and anaphase bridging in regenerating mTR<sup>-/-</sup> livers after partial hepatectomy. (A) Telomere length of peripheral blood lymphocytes determined by Flow-FISH (13) in 8 mTR<sup>+/+</sup> and 10 G6 mTR<sup>-/-</sup> mice before PH. (B) G2/M cell cycle block in regenerating hepatocytes of G6 mTR<sup>-/-</sup> mice 72 hours after PH, as determined by flow cytometry. (C) Delayed progression through mitosis results in an increase in the mitotic index (left) and a shift from prophase to anaphase and metaphase (right) in regenerating livers of G6 mTR<sup>-/-</sup> mice compared with livers from mTR<sup>+/+</sup> mice or G3 mTR<sup>-/-</sup> mice (eight mice per group). (D) Anaphase bridges in H&E-stained regenerating liver sections of G6 mTR<sup>-/-</sup> mice 48 to 96 hours after PH. The arrows point to chromatid bridges between the separating chromosomes. Anaphase from a mTR<sup>+/+</sup> control liver is shown on the left for comparison (bars: 20 μm).

G2 mTR<sup>-/-</sup> mice are telomerase-deficient yet still possess long, intact telomeres (7), it appears that telomerase activity itself is not a key determinant of hepatocyte regeneration potential. In contrast, a decrease in transgene transmission (16% transgene-positive on postnatal day 12) and reciprocal rise in perinatal deaths became evident in G3 mTR<sup>-/-</sup> mice (Fig. 1A). In addition, the few surviving Alb-uPA G3 mTR<sup>-/-</sup> mice exhibited reduced fitness and poor weight gain relative to Alb-uPA mTR<sup>+/+</sup> controls, whereas nontransgenic G3 mTR<sup>-/-</sup> and mTR<sup>+/+</sup> animals were phenotypically indistinguishable (Fig. 1B). Flow-fluorescence in situ hybridization (FISH) telomere length measurements of peripheral blood lymphocytes documented the expected progressive decline in telomere lengths from G1 to G3 (7, 13).

To assess clonal liver regeneration potential in the surviving Alb-uPA transgenic mice, we monitored the growth of regenerative liver nodules, which are estimated to arise from about 20 cell doublings of a single transgene-negative hepatocyte (11). Impaired growth of regenerative nodules in the Alb-uPA G3 mTR<sup>-/-</sup> livers was first detectable by 2 weeks of age and most pronounced by week 4 (Fig. 1C). The impaired macroscopic growth of regenerative nodules in mice with shorter telomeres correlated with a 3.6-fold increase in TUNEL (terminal deoxynucleotidyl transferase dUTP nick-end labeling)-positive apoptotic cells in the regenerative nodules (Fig. 1D, top) (P = 0.003) and a decrease in proliferating cell nuclear antigen (PCNA)-positive S phase cells (Fig. 1D, bottom).

The second approach we used to test liver regenerative capacity was partial hepatectomy (PH), surgical removal of two-thirds of

## REPORTS

the liver (14). In this procedure greater than 50% of hepatocytes follow a highly synchronized cell cycle reentry pattern, reaching peak S-phase activity at 24 to 48 hours, maximal mitosis at 72 hours, and cessation of cell division at 96 hours after PH. After this regenerative wave, normal organ histology is reestablished within 1 week (15). Consistent with the shorter telomere length of G6 mTR<sup>-/-</sup> mice (Fig. 2A), the liver mass of G6 mTR<sup>-/-</sup> mice at 72 hours after PH was reduced relative to mTR<sup>+/+</sup> controls, despite comparable liver weight in G6 mTR<sup>-/-</sup> and mTR<sup>+/+</sup> mice not subjected to PH (9). In addition, although all mTR<sup>+/+</sup> mice were found to be free of lethal postoperative complications, 3 of the 10 G6 mTR<sup>-/-</sup> mice died 48 to 72 hours after PH. Interestingly, these compromised mice had shorter telomeres than the G6 mTR<sup>-/-</sup> survivors (9).

The impaired regeneration of post-PH livers of surviving G6 mTR<sup>-/-</sup> mice prompted us to analyze the regenerative profile of G6 mTR<sup>-/-</sup> hepatocytes by flow cytometry, mitotic index determination, and bromodeoxyuridine labeling. These cells showed a normal onset of S phase at 24 hours after PH (9). In contrast, at 72 hours after PH, flow cytometry of cells from the regenerating liver front (16) revealed a two- to threefold increase in the G<sub>2</sub>/M fraction of G6 mTR<sup>-/-</sup> hepatocytes relative to mTR<sup>+/+</sup> and G3 mTR<sup>-/-</sup> controls (Fig. 2B). This effect was also apparent microscopically as an increase in the number of mitotic figures (Fig. 2C). Further classification of the mitotic profile demonstrated a decrease in the prophase fraction and a compensatory increase in the metaphase/anaphase fraction (Fig. 2C). These data are consistent with impaired cell progression through mitosis, as opposed to a higher number of cells entering mitosis. We propose that telomere loss may interfere with progression through mitosis because of the production of end-to-end chromosomal fusions, opposing kinetochore alignment, and anaphase bridges (17). Indeed, hematoxylin and eosin (H&E)-stained liver sections at 48 to 96 hours after PH showed many aberrant mitotic figures and anaphase bridges only in the G6 mTR<sup>-/-</sup> liver samples (Fig. 2D). Together, these findings indicate that telomere dysfunction delays the mitotic progression of regenerating G6 mTR<sup>-/-</sup> hepatocytes and in turn delays the restoration of liver mass after surgical hepatectomy.

The third approach we used to assess the impact of telomere dysfunction on liver regeneration was repeated toxin-mediated liver injury, which is known to culminate in liver cirrhosis. In humans, cirrhosis often results from the accumulated effects of years of sustained hepatocyte destruction and subsequent regeneration. This can be modeled in mice by repeated exposure to hepatotoxins such as

CCl<sub>4</sub> (18). In mice, 12 to 18 repeated applications of CCl<sub>4</sub> are required to induce modest liver cirrhosis, which is thought to be mechanistically linked to hepatocyte necrosis (18). Given the long length of mouse telomeres (19), the promiscuous somatic expression of telomerase in the mouse liver, and the limited number of cell divisions after CCl<sub>4</sub> treatment, the mTR<sup>-/-</sup> mouse affords a system in which to test whether telomere dysfunction limits hepatocyte function and accelerates the development of liver cirrhosis.

One consistent feature of the cirrhotic patient is poor weight gain due to several factors including hypermetabolism, malabsorption, recurrent infections, and poor appetite (20). Another feature of the cirrhotic condition is impaired bile drainage (cholestasis), leading to persistently elevated serum bilirubin levels and jaundice (21). After 3 months of CCl<sub>4</sub> treatment (22), the G6 mTR<sup>-/-</sup> mice showed significantly impaired gain of body weight compared with mTR<sup>+/+</sup> or G3 mTR<sup>-/-</sup> mice. After 6 months of CCl<sub>4</sub> administration, poor weight gain persisted in G6 mTR<sup>-/-</sup> mice and became manifest in G3 mTR<sup>-/-</sup> mice as well (Fig. 3A). Marked increases of serum bilirubin levels were also seen in the G6 mTR<sup>-/-</sup> mice after only two rounds of CCl<sub>4</sub> (Fig. 3B). Finally, liver sections of

mTR<sup>+/+</sup> and G3 mTR<sup>-/-</sup> mice, treated with six rounds of CCl<sub>4</sub>, exhibited mild lipid accumulation (steatosis) and minimal fibrosis (Fig. 3C), whereas comparable sections from G6 mTR<sup>-/-</sup> mice showed pronounced steatosis, centrilobular fibrosis, and inflammatory lymphocytic infiltrates—hallmarks of chronic hepatic injury and cirrhosis (Fig. 3C).

To determine if telomerase administration could block the development of cirrhosis in mice with dysfunctional telomeres, we constructed adenoviral vectors that would direct the expression of GFP (green fluorescent protein) alone or mTR-GFP to the livers of mTR<sup>+/+</sup> and G6 mTR<sup>-/-</sup> mice (23). In these studies, we verified that the mean telomere length in lymphocytes of G6 mTR<sup>-/-</sup> mice was ~70% reduced compared with that of mTR<sup>+/+</sup> mice (Fig. 4A). Forty-eight hours after delivery of 1 × 10<sup>12</sup> viral particles by tail vein injections, telomerase activity was detected in the liver but not in the spleen of G6 mTR<sup>-/-</sup> mice infected with the Ad-mTR-GFP virus (Fig. 4B, compare lane 5 with lane 4), consistent with the strong liver tropism of adenovirus (24). Liver cryosections obtained at the same time demonstrated GFP fluorescence in 85 to 100% of liver cells.

We next examined whether cirrhosis could be inhibited in G6 mTR<sup>-/-</sup> mice by

**Fig. 3.** Telomere shortening accelerates the development of cirrhosis in response to chronic liver damage. (A) Reduced body-weight gain in G6 mTR<sup>-/-</sup> mice compared with G3 mTR<sup>-/-</sup> and mTR<sup>+/+</sup> mice after repeated liver injury (monthly injections of 10 μl of 10% CCl<sub>4</sub> per gram of body weight), with six mice examined per group. (B) A twofold increase of serum bilirubin in G6 mTR<sup>-/-</sup> mice compared with similarly treated G3 mTR<sup>-/-</sup> and mTR<sup>+/+</sup> mice (six mice per group) was seen after the second injection of CCl<sub>4</sub>. (C) H&E-stained (upper; bar: 50 μm) and Masson-trichrome-stained (lower; bar: 100 μm) liver sections of mTR<sup>+/+</sup>, G3 mTR<sup>-/-</sup>, and G6 mTR<sup>-/-</sup> mice 6 months after repeated CCl<sub>4</sub>-induced liver injury. Marked steatosis (vacuolated appearance) and fibrosis (blue stain with Masson-trichrome, arrows) are evident in livers of G6 mTR<sup>-/-</sup> mice but not in livers of mTR<sup>+/+</sup> and G3 mTR<sup>-/-</sup> mice. (Inset) High-power view of collagen deposition (blue stain) in the centrilobular areas of G6 mTR<sup>-/-</sup> mice (bar: 50 μm).

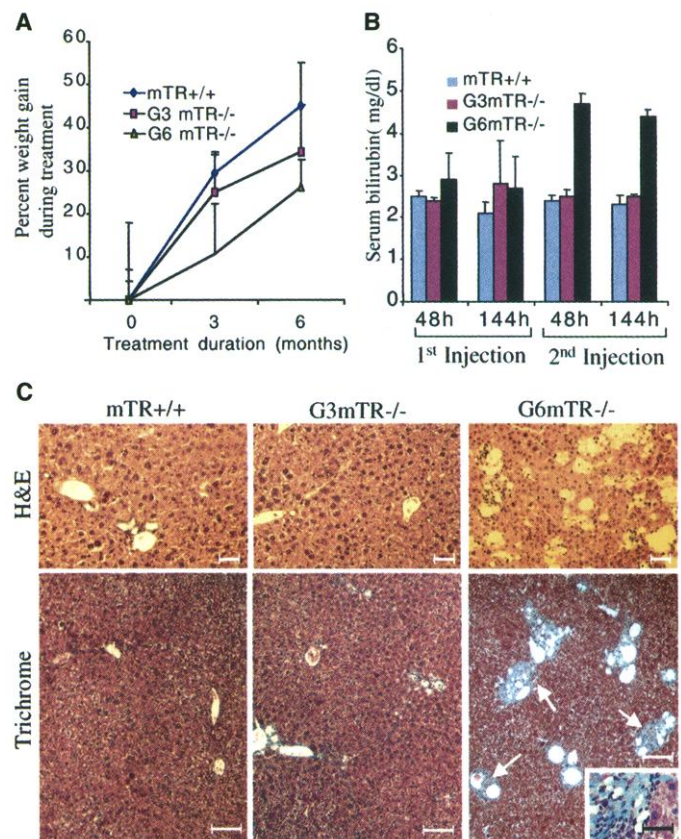
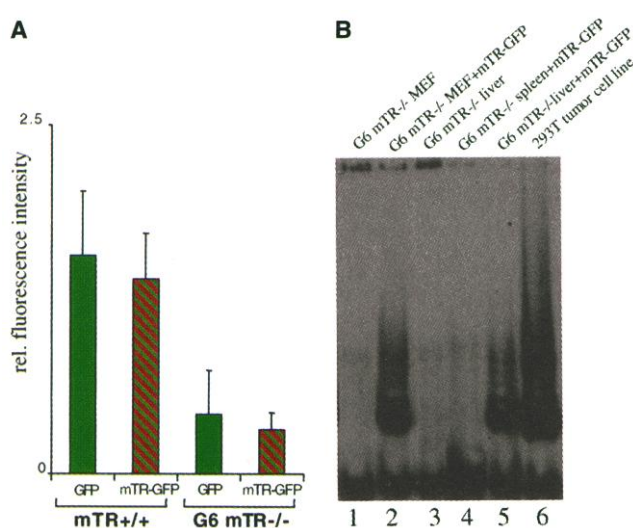
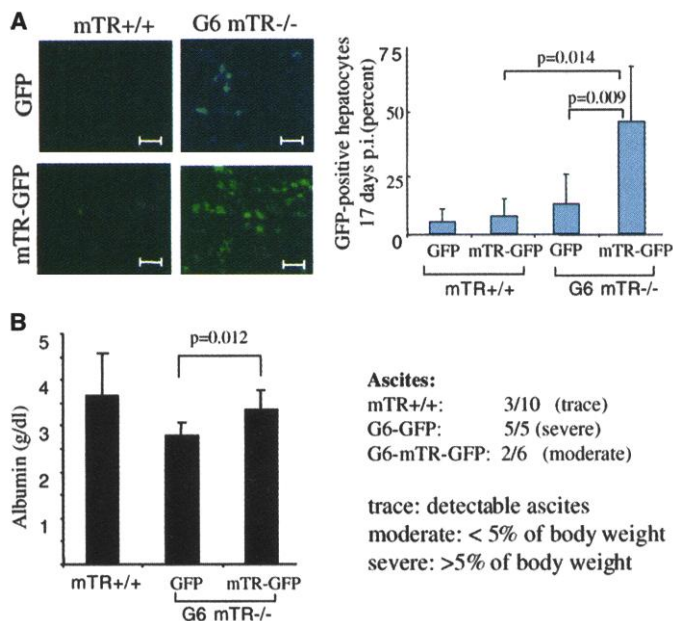


**Fig. 4.** Adenovirus-mediated mTR gene transfer restores telomerase activity in the liver of mTR<sup>-/-</sup> mice. (A) Average telomere length (13) of white blood cells obtained from 12 G6 mTR<sup>-/-</sup> and 16 mTR<sup>+/+</sup> mice, which were treated either with mTR-GFP or GFP-expressing adenovirus. (B) Adeno-mTR-GFP infection restores telomerase activity [as determined by the TRAP (telomeric repeat amplification protocol) assay] in G6 mTR<sup>-/-</sup> mouse embryo fibroblasts (compare lane 2 to lane 1) and in the liver of adult G6 mTR<sup>-/-</sup> mice (compare lane 5 to lane 3) 48 hours after infection.



No restoration of telomerase activity was seen in the spleen of Ad-mTR-GFP-infected mice (lane 4). Telomerase activity of 293 cells was assessed as a positive control (lane 6).

**Fig. 5.** Reactivation of telomerase improves liver function in G6 mTR<sup>-/-</sup> mice. (A) (Left) GFP immunofluorescence of liver cryosections (bar: 100 μm). Hepatocytes of mTR<sup>+/+</sup> mice infected with both Ad-GFP and Ad-mTR-GFP were rapidly lost 2 weeks after infection, whereas continuous expression was seen in Ad-mTR-GFP-infected hepatocytes of G6 mTR<sup>-/-</sup> mice. (Right) Quantitation of GFP expression in hepatocytes 17 days postinfection (p.i.), as determined in five mice per experimental group. (B) (Left) Decreased serum albumin in Ad-GFP-G6 mTR<sup>-/-</sup> mice compared with mTR<sup>+/+</sup> mice and Ad-mTR-GFP-G6 mTR<sup>-/-</sup> mice, 4 weeks after alternate day CCl<sub>4</sub> treatment (data are from six to eight mice per experimental group). (Right) Frequency and severity of ascites after 4 weeks of alternate-day CCl<sub>4</sub> treatment, determined at the time of surgical biopsies of the liver.



this gene therapy approach. Two days before initiation of repeated alternate-day CCl<sub>4</sub> injections, mTR<sup>+/+</sup> and G6 mTR<sup>-/-</sup> mice were infected with Ad-mTR-GFP or Ad-GFP (25). At 17 days after infection, ~45% of liver cells in Ad-mTR-GFP-infected G6 mTR<sup>-/-</sup> mice were GFP-positive, whereas <10% were GFP-positive in Ad-GFP-infected mTR<sup>+/+</sup> and G6 mTR<sup>-/-</sup> mice, or in Ad-mTR-GFP-infected mTR<sup>+/+</sup> mice (Fig. 5A). These data suggest that there was positive selection of mTR-GFP-expressing cells in the livers of G6 mTR<sup>-/-</sup> mice.

If restoration of telomerase activity con-

fers a growth advantage to G6 mTR<sup>-/-</sup> hepatocytes, then it should improve the regenerative capacity and phenotypic outcome of G6 mTR<sup>-/-</sup> mice subjected to chronic liver damage. Severe (>5% of body weight) accumulation of peritoneal fluid (ascites, a clinical hallmark of advanced liver cirrhosis) (26) was observed in 5 of 5 G6 mTR<sup>-/-</sup> mice after 4 weeks of CCl<sub>4</sub> treatment, whereas only 3 out of 10 mTR<sup>+/+</sup> mice exhibited trace ascites at this time point (Fig. 5B). When infected with Ad-mTR-GFP, only 2 of 6 G6 mTR<sup>-/-</sup> mice showed modest ascites. These data matched an acute 13% increase

in body weight in Ad-GFP-infected G6 mTR<sup>-/-</sup> mice compared with a 6% increase in Ad-mTR-GFP-infected G6 mTR<sup>-/-</sup> mice. Moreover, the severity of ascites was inversely correlated with serum albumin levels (Fig. 5B). Albumin is a major product of hepatocytes and a critical serum protein required for the maintenance of vascular oncotic pressure and fluid homeostasis; thus, these findings are consistent with improved liver function after telomerase treatment.

Histological examinations of liver sections 2 weeks after CCl<sub>4</sub> treatment showed fibrosis in combination with increased steatosis, pericentral necrosis, and a marked increase in both cell and nuclear size only in livers of Ad-GFP-infected G6 mTR<sup>-/-</sup> mice (Fig. 6A, top). After prolonged exposure to CCl<sub>4</sub> (4 weeks), mild fibrosis also developed in livers of mTR<sup>+/+</sup> and mTR-rescued G6 mTR<sup>-/-</sup> mice (Fig. 6A, bottom). Our observations that serum levels of alanine aminotransferase and aspartate aminotransferase in response to CCl<sub>4</sub> treatment are equal in mTR<sup>+/+</sup> and G6 mTR<sup>-/-</sup> mice suggest that the extent of CCl<sub>4</sub>-induced hepatic necrosis was not significantly affected by telomere shortening.

A strong correlation between decreased cell proliferation and progression of human liver cirrhosis has been described (3). In the liver of G6 mTR<sup>-/-</sup> mice infected with Ad-GFP, minimal hepatocyte proliferation, as measured by immunohistochemistry with the proliferation marker PCNA (27), was observed 2 weeks after continuous exposure to CCl<sub>4</sub> (Fig. 6B). (Fig. 6B). In contrast, Ad-mTR-GFP-infected G6 mTR<sup>-/-</sup> mice showed high rates of hepatocyte proliferation (comparable to that seen in the mTR<sup>+/+</sup> mice) (Fig. 6B) (27). There was a 66% decrease in the mitotic index and a 58% decrease in anaphase bridges in Ad-mTR-GFP-infected G6 mTR<sup>-/-</sup> mice as compared with Ad-GFP-infected G6 mTR<sup>-/-</sup> mice. Thus, delivery of the telomerase RNA gene rescues telomerase dysfunction and impaired hepatocyte proliferation in G6 mTR<sup>-/-</sup> mice.

TGF-β1 has been identified as a major factor stimulating stellate cell fibrogenic activity, a hallmark of human liver cirrhosis (4). After 2 weeks of repeated CCl<sub>4</sub> injury, increased TGF-β1 staining was present in liver sections of Ad-GFP-infected G6 mTR<sup>-/-</sup> mice as compared with Ad-mTR-GFP-infected G6 mTR<sup>-/-</sup> mice (Fig. 6C). TGF-β1 was predominantly expressed in centrilobular areas and correlated with an enhanced number of α-smooth muscle antigen and desmin-positive cells, both markers of activated stellate cells (Fig. 6D) (2, 27).

In conclusion, these results underscore the importance of the regenerating hepatocyte in the pathogenesis of liver cirrhosis and forge a pathogenic chain of events from telomere dysfunction to anaphase bridges to impaired

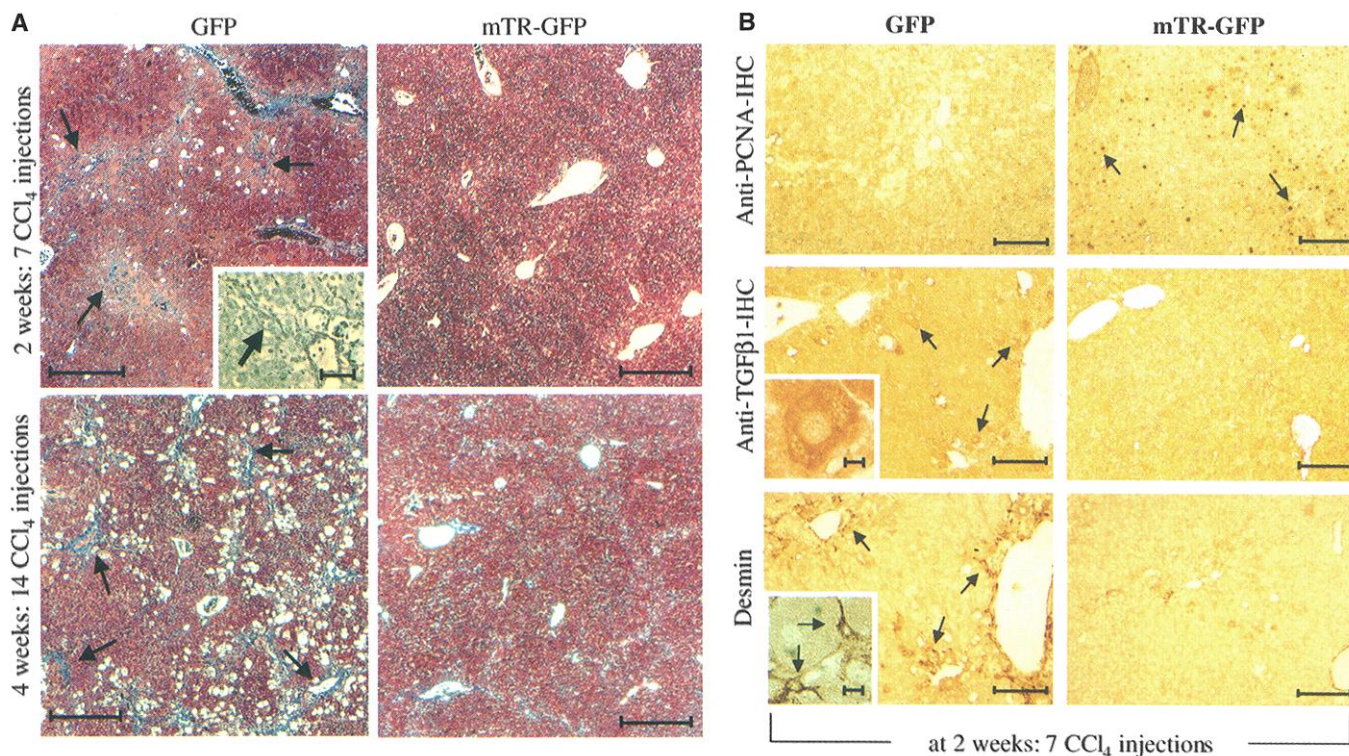


**Fig. 6.** Reactivation of telomerase reduces liver cirrhosis in G6 mTR<sup>-/-</sup> mice. **(A)** Masson-Trichrome stains 2 and 4 weeks after repeated CCl<sub>4</sub> treatment showed accelerated fibrosis (arrows) in Ad-GFP-treated G6 mTR<sup>-/-</sup> mice as compared with Ad-mTR-GFP-treated G6 mTR<sup>-/-</sup> mice (bar: 200 μm). **(Inset)** Reticulin staining of pericentral fibrosis (arrow) in Ad-GFP-treated G6 mTR<sup>-/-</sup> mice (bar: 50 μm). Enhanced steatosis is apparent in Ad-GFP-treated G6 mTR<sup>-/-</sup> mice. **(B)** PCNA staining (top) showed decreased hepatocyte proliferation in chronically injured livers of Ad-GFP-treated G6 mTR<sup>-/-</sup> mice as compared with Ad-mTR-GFP-

treated G6 mTR<sup>-/-</sup> mice (arrows point to PCNA-positive cells; bar: 100 μm). Increased TGF-β1 immunoreactivity (middle) is evident in centrilobular areas of Ad-GFP-treated G6 mTR<sup>-/-</sup> mice (arrows) but not in Ad-mTR-GFP-treated G6 mTR<sup>-/-</sup> mice (bar: 100 μm). **(Inset)** Typical cytoplasmic localization of TGF-β within cells (bar: 10 μm). An increased number of desmin-positive stellate cells (bottom) in Ad-GFP-treated mice (arrows); in contrast, Ad-mTR-GFP-treated mice showed only background staining of endothelial cells of hepatic vessels (bar: 100 μm). **(Inset)** Typical morphology of desmin-positive stellate cells (bar: 10 μm).

liver regeneration. The development of anaphase bridges in hepatocytes and subsequent double-strand DNA breaks could initiate DNA damage responses, resulting in growth arrest and increased apoptosis. Liberation of lipid peroxides (formed by dying hepatocytes) and/or activation of cell cycle inhibitors such as TGF-β1 could promote stellate cell activation leading to fibrosis. In addition, telomere shortening might alter the ability of cells to cope with various stresses (e.g., diminished oxidative stress capacity), possibly resulting in increased hepatocyte death typical of end-stage chronic liver disease.

Our study indicates that telomere shortening contributes to the pathogenesis of liver cirrhosis and that telomerase therapy may be beneficial for this disease. Can we extend these animal-based findings to humans? The significant reduction in telomere length seen in human cirrhotic livers is well within the range associated with activation of cellular senescence and the onset of genetic instability (28). In the mouse, telomere attrition is associated more often with crisis than with replicative senescence (7, 29). However, both responses converge upon common physiological end points that affect the ability of hepa-

tocytes to sustain robust regenerative responses after injury. On this basis, it is reasonable to anticipate that activation of telomerase could inhibit the development of liver cirrhosis or terminal liver failure in humans.

As a caveat, the possible adverse effects of telomerase reactivation will have to be considered, particularly given the correlation between telomerase overexpression and cancer pathogenesis (30). Over 80% of hepatomas exhibit telomerase activity (31), suggesting that telomerase reactivation could facilitate tumor formation in the liver. In contrast, the increased cancer incidence we have observed in aging mTR<sup>-/-</sup> mice (8) indicates that activation of telomerase might act as a double-edged sword in terms of genomic instability and tumor formation. In addition, a transient activation of the enzyme (as in our gene transfer experiments) may be insufficient to facilitate the clonal expansion of single transformed cells required for tumor formation. From a clinical point of view, patients with end-stage liver cirrhosis awaiting liver transplantation might be ideal candidates for telomerase therapy, because telomerase-mediated improvement in liver function could extend survival, and the even-

tual surgical removal of the organ should minimize potential cancer risk.

Finally, the liver's wound healing response is a paradigm for how other organ systems might respond to the stress of long-standing cell depletion and renewal. Thus, in principle, the pathophysiological and therapeutic insights gained from the study of liver cirrhosis may be applicable to other chronic high-turnover disease states such as immunosenescence in advanced human immunodeficiency virus infection (32) and bone-marrow exhaustion in myeloproliferative diseases (33).

**References and Notes**

1. R. G. Smart, R. E. Mann, H. J. Suurvali, *J. Stud. Alcohol* **59**, 245 (1998); R. G. Smart, R. E. Mann, S. L. Lee, *Alcohol Alcohol* **31**, 487 (1996); *Morbid. Mortal. Wkly. Rep.* **41**, 969 (1993); R. G. Smart and R. E. Mann, *J. Stud. Alcohol* **52**, 232 (1991); [www.niddk.nih.gov/health/digest/pubs/cirrhosi/cirrhosi.htm](http://www.niddk.nih.gov/health/digest/pubs/cirrhosi/cirrhosi.htm).
2. S. L. Friedman, *N. Engl. J. Med.* **328**, 1828 (1993); E. J. Williams and J. P. Iredale, *Postgrad. Med. J.* **870**, 193 (1998); R. Alcolado, M. J. P. Arthur, J. P. Iredale, *Clin. Sci.* **92**, 103 (1997).
3. M. Delhaye et al., *Hepatology* **23**, 1003 (1996).
4. D. Roulot, A. M. Sevcik, T. Coste, A. D. Strosberg, S. Marullo, *Hepatology* **29**, 1730 (1999); N. Fausto, J. E. Mead, P. A. Gruppiso, A. Castilla, S. B. Jakowlew, *Ciba Found. Symp.* **157**, 165 (1991); P. Bedossa, E. Peltier,

- B. Terris, D. Franco, T. Poynard, *Hepatology* **21**, 760 (1995); S. Milani, H. Herbst, D. Schuppan, H. Stein, C. Surrenti, *Am. J. Pathol.* **139**, 1221 (1991).
5. T. Kitada, S. Seki, N. Kawakita, T. Kuroki, T. Monna, *Biochem. Biophys. Res. Commun.* **211**, 33 (1995); N. Miura et al., *Cancer Genet. Cytogenet.* **93**, 56 (1997); Y. Urabe et al., *Liver* **16**, 293 (1996).
6. A. G. Bodnar et al., *Science* **279**, 349 (1998); H. Vaziri and S. Benchimol, *Curr. Biol.* **8**, 279 (1998); C. M. Counter, *Mutat. Res.* **366**, 45 (1996); T. Kiyono et al., *Nature* **396**, 84 (1998).
7. M. A. Blasco et al., *Cell* **91**, 25 (1997).
8. H. W. Lee et al., *Nature* **392**, 569 (1998); K. L. Rudolph et al., *Cell* **96**, 701 (1999).
9. K. L. Rudolph, S. Chang, M. Millard, N. Schreiber-Agus, R. A. DePinto, unpublished data.
10. J. L. Heckel, E. P. Sandgren, J. L. Degen, R. D. Palmiter, R. L. Brinster, *Cell* **62**, 447 (1990).
11. E. P. Sandgren et al., *Cell* **66**, 245 (1991).
12. Mice homozygous null for the mouse telomerase RNA gene (mTR<sup>-/-</sup>) were bred to transgenic mice hemizygous for the Alb-uPA transgene. Alb-uPA mTR<sup>+/-</sup> mice were crossed to mTR<sup>+/-</sup> mice, generating Alb-uPA mTR<sup>-/-</sup> mice (G1). Intercrosses of Alb-uPA mTR<sup>-/-</sup> mice according to previously published mating schemes (7) resulted in successive generations of Alb-uPA mTR<sup>-/-</sup> mice.
13. N. Rufer, W. Dragowska, G. Thornbury, E. Roosnek, P. M. Lansdorp, *Nature Biotechnol.* **16**, 743 (1998).
14. PH was performed as described (15). Briefly, mice were anesthetized by intraperitoneal (i.p.) injections of 2.5% Avertin. After ligation of the blood supply and resection of the left and the left-anterior lobes of the liver, the abdominal cavity was closed with peritoneal and dermal sutures. Regenerating livers were removed at the indicated time points, photographed with a Nikon 2000 camera, and fixed in 10% phosphate-buffered saline (PBS)-buffered formalin for histology.
15. K. L. Rudolph et al., *Hepatology* **30**, 1159 (1999); A. M. Diehl and R. M. Rai, *FASEB J.* **10**, 215 (1996).
16. Single-cell suspensions of regenerating livers were produced by homogenizing the organs between two glass slides. Homogenates were then filtered through a nylon mesh (60- $\mu$ m opening; Sefor America, Kansas City, MO). After several washes with ice-cold PBS, single-cell suspensions were fixed in 70% ethanol and stained with propidium iodide.
17. B. McClintock, *Genetics* **26**, 234 (1941); B. van Steensel, A. Smorzewska, T. de Lange, *Cell* **92**, 401 (1998); E. Blackburn et al., *Ciba Found. Symp.* **211**, 2 (1997); K. E. Kirk, B. P. Harmon, I. K. Reichardt, J. W. Sedat, E. H. Blackburn, *Science* **275**, 1478 (1997).
18. R. P. Tamayo, *Hepatology* **3**, 112 (1983).
19. K. R. Prox and C. W. Greider, *Proc. Natl. Acad. Sci. U.S.A.* **92**, 4818 (1995).
20. D. K. Podolsky and K. J. Isselbacher, in *Harrison's Principles of Internal Medicine*, A. S. Fauci et al., Eds. (McGraw-Hill, New York, ed. 14, 1998), p. 1704.
21. P. P. Anthony et al., *Bull. WHO* **55**, 521 (1977).
22. Ten microliters of 10% CCl<sub>4</sub> in olive oil were injected into mice i.p. once per month starting with 6-week-old animals. Peripheral bleeds were performed 48 hours and 144 hours after CCl<sub>4</sub> injections. Liver biopsies were taken 1 month after the sixth injection of CCl<sub>4</sub>. Formalin-fixed, paraffin-embedded liver sections were stained with Masson-trichrome, H&E, and reticulin.
23. A 5-kb Eco RI fragment of mTR including 4 kb of the upstream promoter region was cloned into the pAdTrack-Shuttle vector (24). Homologous recombination of Pme I-linearized pAdTrack-mTR DNA with the viral backbone vector pAd-Easy-1 (24) was performed in *Escherichia coli* BJ5183 cells, yielding a replication-deficient (lack of E1/3) Ad5-mTR-virus. Virus was grown in 293 cells and purified as in (24).
24. T. C. He et al., *Proc. Natl. Acad. Sci. U.S.A.* **95**, 2509 (1998).
25. Six- to eight-week-old mTR<sup>+/+</sup> and G6 mTR<sup>-/-</sup> mice were infected with 10<sup>12</sup> virus particles of Ad-mTR-GFP or Ad-GFP by tail-vein injections. Two days after injection, liver biopsies were performed and GFP expression was monitored on unstained, 5- $\mu$ m-thick cryostat sections. Subsequent alter-
- nate-day CCl<sub>4</sub> i.p. injections were administered (10  $\mu$ l of 10% CCl<sub>4</sub> per gram of body weight in olive oil). Liver biopsies for both GFP expression and histology were performed 14 and 28 days after initiation of the CCl<sub>4</sub> injections.
26. J. Korula, in N. Kaplowitz, Ed., *Liver and Biliary Diseases* (Williams & Wilkins, Baltimore, MD, 1992), pp. 529-541.
27. For immunostaining, 10- $\mu$ m paraffin liver sections were incubated overnight at 4°C with 1:100 dilutions of the primary antibody (mouse anti-PCNA or mouse anti-TGF- $\beta$ 1) in the presence of 1.5% goat serum. The Elite Vectastain ABC kit (Vector Labs) was used for subsequent peroxidase substrate detection. Stained sections were dehydrated and mounted in Permount.
28. C. B. Harley, A. B. Fletcher, C. W. Greider, *Nature* **345**, 458 (1990); C. Mondello, R. Riboni, A. Casati, T. Nardo, F. Nuzzo, *Exp. Cell Res.* **236**, 385 (1997); C. Pan, B. H. Xue, T. M. Ellis, D. J. Peace, M. O. Diaz, *Exp. Cell Res.* **231**, 346 (1997); R. C. Allsopp and C. B. Harley, *Exp. Cell Res.* **219**, 130 (1995).
29. H. Niida et al., *Nature Genet.* **19**, 203 (1998); L. Chin et al., *Cell* **97**, 527 (1999).
30. R. A. Greenberg et al., *Cell* **97**, 515 (1999); W. C. Hahn et al., *Nature* **400**, 464 (1999); J. W. Shay, *J. Cell. Physiol.* **173**, 266 (1997); C. B. Harley et al., *Cold Spring Harbor Symp. Quant. Biol.* **59**, 307 (1994); T. de Lange, *Proc. Natl. Acad. Sci. U.S.A.* **91**, 2882 (1994).
31. H. Tahara et al., *Cancer Res.* **55**, 2734 (1995); G. T. Huang et al., *Eur. J. Cancer* **34**, 1946 (1998); Y. M. Park et al., *Exp. Mol. Med.* **30**, 35 (1998); R. Nakishio, M. Kitamoto, T. Nakaishi, H. Takahashi, G. Kajiyama, *Nippon Rinsho* **56**, 1239 (1998); T. Suda et al., *Hepatology* **27**, 402 (1998); H. Kojima, O. Yokosuka, F. Imazeki, H. Saisho, M. Omata, *Gastroenterology* **112**, 493 (1997).
32. J. P. Pommier et al., *Virology* **231**, 148 (1997); W. S. Nichols, S. Schneider, R. C. Chan, C. F. Farthing, E. S. Daar, *Scand. J. Immunol.* **49**, 302 (1999).
33. J. H. Ohyashiki et al., *Clin. Cancer Res.* **5**, 1155 (1999); S. E. Ball et al., *Blood* **91**, 3582 (1998); J. H. Ohyashiki et al., *Cancer Res.* **54**, 3557 (1994).
34. We thank I. Arias, G. Merlino, M. Meyerson, N. Sharpless, and G. David for critical reading of the manuscript; B. Vogelstein for the Ad-Easy-Adenovirus-System; J. Furgiueli for serum chemistry analysis; and V. V. Lam for technical assistance. Supported by Deutsche Forschungsgemeinschaft grant Ru 745/1-1 (K.L.R.), Leukemia Society of America fellowship (N.S.-A.), and the Dana-Farber Cancer Institute Cancer Core Grant (R.A.D.). R.A.D. is funded by NIH grants (R01HD34880 and R01HD28317), the American Heart Association Grant-in-Aid, and the American Cancer Society.

8 November 1999; accepted 22 December 1999

## Prevention of Acute Liver Failure in Rats with Reversibly Immortalized Human Hepatocytes

Naoya Kobayashi,<sup>1\*</sup> Toshiyoshi Fujiwara,<sup>1</sup> Karen A. Westerman,<sup>2</sup> Yusuke Inoue,<sup>3</sup> Masakiyo Sakaguchi,<sup>3</sup> Hirofumi Noguchi,<sup>1</sup> Masahiro Miyazaki,<sup>3</sup> Jin Cai,<sup>4</sup> Noriaki Tanaka,<sup>1</sup> Ira J. Fox,<sup>4\*</sup> Philippe Leboulch<sup>2,5\*</sup>

Because of a critical shortage in suitable organs, many patients with terminal liver disease die each year before liver transplantation can be performed. Transplantation of isolated hepatocytes has been proposed for the temporary metabolic support of patients awaiting liver transplantation or spontaneous reversion of their liver disease. A major limitation of this form of therapy is the present inability to isolate an adequate number of transplantable hepatocytes. A highly differentiated cell line, NKNT-3, was generated by retroviral transfer in normal primary adult human hepatocytes of an immortalizing gene that can be subsequently and completely excised by Cre/Lox site-specific recombination. When transplanted into the spleen of rats under transient immunosuppression, reversibly immortalized NKNT-3 cells provided life-saving metabolic support during acute liver failure induced by 90% hepatectomy.

Orthotopic allogeneic liver transplantation remains the only treatment option available to patients with terminal liver failure or inborn errors of liver metabolism. Because its application is limited by donor organ availability, considerable morbidity, mortality, and high cost, there is a need to develop bridging procedures to sustain patients with subacute or acute liver failure. Hepatocyte transplantation (HTX) has been used to correct metabolic defects and provide metabolic support in experimental animal models of hepatic fail-

ure (1). The hyperbilirubinemia of rats genetically deficient in uridine diphosphate glucuronosyltransferase was corrected by HTX (1). Substantial increases in plasma albumin levels were also documented after HTX into analbuminemic rats (1). Recently, intrasplenic transplantation of differentiated adult hepatocytes in human patients with severe encephalopathy and multisystem organ failure was able to control hyperammonemia and ensure short-term survival until orthotopic liver transplantation was successfully per-